Missouri University of Science and Technology
Scholars' Mine

Electrical and Computer Engineering Faculty Research & Creative Works

Electrical and Computer Engineering

01 Jan 1982

Conversion And Matched Filter Approximations For Serial Minimum-Shift Keyed Modulation

Carl R. Ryan

James H. Stilwell

Rodger E. Ziemer
Missouri University of Science and Technology

Follow this and additional works at: https://scholarsmine.mst.edu/ele_comeng_facwork

Part of the Electrical and Computer Engineering Commons

Recommended Citation

C. R. Ryan et al., "Conversion And Matched Filter Approximations For Serial Minimum-Shift Keyed Modulation," *IEEE Transactions on Communications*, vol. 30, no. 3, pp. 495 - 509, Institute of Electrical and Electronics Engineers, Jan 1982.
The definitive version is available at https://doi.org/10.1109/TCOM.1982.1095489

This Article - Journal is brought to you for free and open access by Scholars' Mine. It has been accepted for inclusion in Electrical and Computer Engineering Faculty Research & Creative Works by an authorized administrator of Scholars' Mine. This work is protected by U. S. Copyright Law. Unauthorized use including reproduction for redistribution requires the permission of the copyright holder. For more information, please contact scholarsmine@mst.edu.

Conversion and Matched Filter Approximations for Serial Minimum-Shift Keyed Modulation

RODGER E. ZIEMER, SENIOR MEMBER, IEEE, CARL R. RYAN, SENIOR MEMBER, IEEE, AND JAMES H. STILWELL, MEMBER, IEEE

Abstract—**Serial minimum-shift keyed (MSK) modulation, a technique for generating and detecting MSK using series filtering, is ideally suited for high data rate applications provided the required conversion and matched filters can be closely approximated. Low-pass implementations of these filters as parallel inphase- and quadrature-mixer structures are characterized in this paper in terms of signal-to-noise ratio (SNR) degradation from ideal and envelope deviation. Several hardware implementation techniques utilizing microwave devices or lumped elements are presented. Optimization of parameter values results in realizations whose SNR degradation is less than 0.5 dB at error probabilities of 10^{-6}.**

I. INTRODUCTION

MINIMUM-shift keyed (MSK) modulation has received considerable attention over the past decade due to its potential as a bandwidth and power efficient constant-envelope modulation technique [1]-[5]. Two generic techniques for the modulation and demodulation of MSK are referred to as the parallel [2], [4] and serial [3], [5] methods. Both are completely equivalent in terms of bandwidth occupancy and bit error rate (BER) performance.

The parallel method amounts to quadrature multiplexing half-sinusoid pulse-shaped data streams staggered by a one-half symbol period on quadrature carriers. Practical implementation of MSK modems employing the parallel approach requires close balancing and alignment of the inphase- and quadrature-channel data signals on carriers which are themselves balanced and in phase quadrature. Similarly, at the receiver, careful balancing and maintenance of phase quadrature is required to minimize distortion and, in particular, crosstalk.

On the other hand, with the series approach, the MSK signal is produced from a biphase signal by filtering it with an appropriately designed conversion filter. The problems of balancing and maintaining phase quadrature carriers of the parallel approach are therefore replaced with the task of building the conversion filter which, ideally, has a sin $(x)/x$ frequency response. Similar to the serial modulator, a serial demodulator is composed of a filter matched to the transmitted signal spectrum, followed by coherent demodulation and bit detection. Implementation of a serial demodulator therefore requires the synthesis of a bandpass filter which is closely matched to the MSK signal in order to ensure performance close to the ideal.

Various approaches have been taken to building serial MSK conversion and matched filters, including the use of surface acoustic wave (SAW) devices [6]. Such devices are limited in bandwidth to roughly 10 percent of their center frequency which is, in turn, limited to a few hundred MHz. Thus, the maximum data rates of SAW-implemented MSK modems are inherently limited to under 100 Mbits/s unless special fabrication techniques are used.

In this paper, the use of baseband equivalents for the conversion and matched filters for serial MSK modems is considered. Such realizations are more suited for high data rate (i.e., in excess of 100 Mbits/s) implementations than SAW devices, do not impose the losses inherent with SAW devices, and may be easily implemented in lumped-element or stripline form.

This paper is arranged as follows. First, the theoretically exact low-pass equivalents for the serial MSK conversion and matched filters are derived and characterized in terms of impulse responses and transfer functions. Second, an approach to realizing these filters as a portion with a periodic frequency response in cascade with a filter which attenuates all but the center lobe of this periodic response is discussed. Two realizations for the portion of the conversion filter with periodic frequency response are discussed next and characterized in terms of signal-to-noise (SNR) ratio degradation and envelope deviation of the modulated signal. Third, approximation of the low-pass equivalent matched filters by means of transversal, or tapped delay line, filters used in conjunction with standard filter types such as Butterworth is considered. This approach not only provides a possible hardware realization, but also a conceptual way of viewing other approximation methods. Several possible realizations using lumped elements or microwave devices are given along with their performances. Last, some results of actual hardware implementations are presented.

The following section, which is somewhat tutorial, provides an important basis for the approximation approach used.

II. LOW-PASS EQUIVALENTS OF SERIAL MSK MODEMS

A. General Discussion

As illustrated in Fig. 1(a), a serial MSK modulator consists of biphase modulation of the data $d(t)$ on a carrier of fre-

Paper approved by the Editor for Radio Communication of the IEEE Communications Society for publication without oral presentation. Manuscript received April 28, 1981; revised September 15, 1981. This work was sponsored by the NASA Lewis Research Center as a part of the "30/20 GHz Communications System Baseband Processor Subsystem" under Contract NAS 3-22502.

R. E. Ziemer is with the Department of Electrical Engineering, University of Missouri–Rolla, Rolla, MO 65401.

C. R. Ryan and J. H. Stilwell are with the Communications Research Facility, Government Electronics Division, Motorola Inc., Gilbert, AZ 85234.

0090-6778/82/0300-0495$00.75 © 1982 IEEE

Authorized licensed use limited to: Missouri University of Science and Technology. Downloaded on July 14,2023 at 19:42:27 UTC from IEEE Xplore. Restrictions apply.

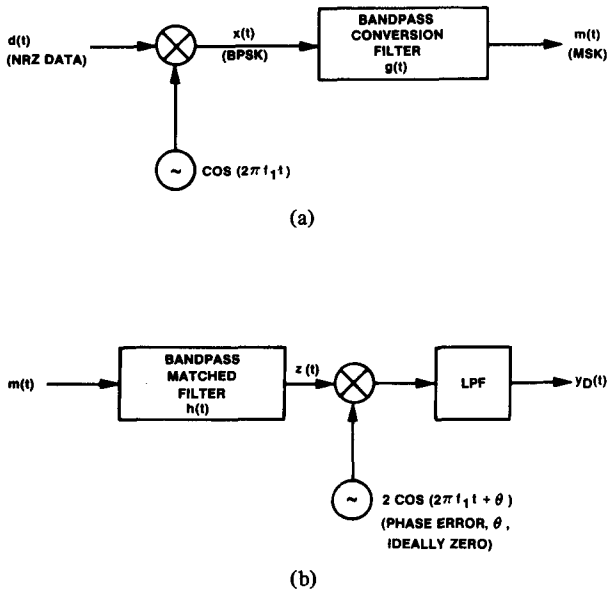

Fig. 1. Implementation of a serial MSK modem utilizing bandpass conversion and matched filters. (a) Modulator. (b) Demodulator.

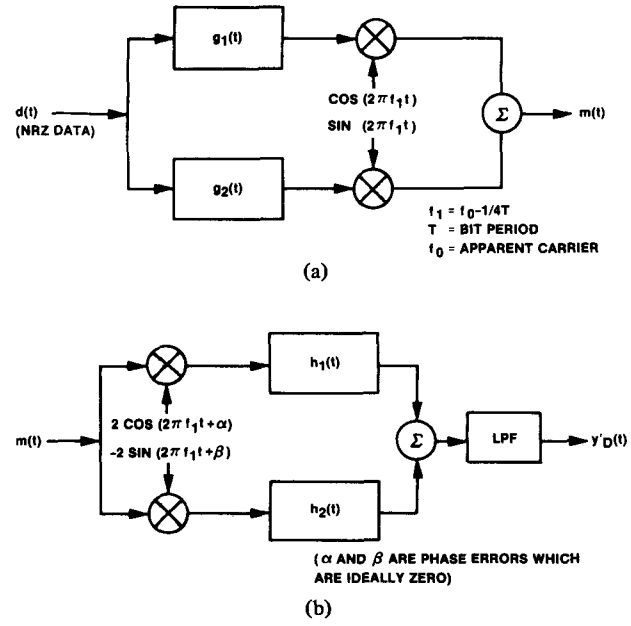

Fig. 2. Implementation of a serial MSK modem utilizing low-pass I/Q equivalents for the conversion and matched filters. (a) Modulator. (b) Demodulator.

quency $f_1 = f_0 - 1/4T$, T being the bit period of $d(t)$, followed by a bandpass conversion filter with impulse response

$$g(t) = \begin{cases} 2 \sin 2\pi f_2 t, & 0 \leqslant t \leqslant T \\ 0, & \text{otherwise} \end{cases} \tag{1}$$

where $f_2 = f_0 + 1/4T$. The frequency response function corresponding to (1) will be given later.

Consistent with previously used terminology, we will refer to f_1, f_2, and f_0 as the mark, space, and apparent carrier frequencies, respectively. The output of the MSK modulator is a sinusoid of frequency f_1 if $d(t)$ is an all 1's or all 0's sequence, and a sinusoid of frequency f_2 if $d(t)$ is an alternating $1 - 0$ sequence.

For a serial MSK demodulator, illustrated in Fig. 1(b), a bandpass filter matched to the transmitted signal is followed by a coherent demodulator which is ideally frequency- and phase-locked to f_1. The actual data detection is then accomplished by sampling at T-second spaced intervals and deciding that a one was sent if a given sample is greater than zero, and a zero otherwise. It has been shown [3] that such a procedure results in a BER performance, under ideal conditions, which is the same as that for a parallel MSK implementation; as a point of reference, a BER of 10^{-6} requires an SNR of about 10.6 dB.

We wish to implement the respective bandpass conversion and matched filters of the serial MSK modulator and demodulator as low-pass equivalents. To this end, we replace the serial modulator and demodulator structures of Fig. 1 with the inphase/quadrature (I/Q) mixer, low-pass filter structures of Fig. 2.[1] From an implementation standpoint, this approach has the following advantageous features.

1) The low-pass filters may be easier to realize at high data rates than bandpass filters.

2) The I/Q mixers can be compactly implemented with a quadrature hybrid supplying the I/Q references from a single local oscillator.

3) Although not evident at this point, the demodulator can be implemented as a Costas loop type of structure by the addition of a single multiplier, thus obtaining carrier synchronization.

We now proceed by demonstrating that the structures of Figs. 1 and 2 can be made equivalent, and discuss the properties of the low-pass filters in the I/Q mixer arms.

B. Conversion Filter Low-Pass Equivalents

In showing the equivalences of the structures of Figs. 1 and 2, it is convenient to use complex envelope notation. For example, for the serial modulator structure, we represent the biphase modulator output, or conversion filter input, in Fig. 1(a) as

$$x(t) = \text{Re}\, d(t) e^{j\omega_1 t} \tag{2}$$

where

$$\omega_1 = 2\pi f_1 = 2\pi(f_0 - 1/4T). \tag{3}$$

We also represent the conversion filter, or MSK modulator, output as

$$m(t) = \text{Re}\, \tilde{m}(t) e^{j\omega_1 t} \tag{4}$$

and the conversion filter impulse response as

$$g(t) = 2\, \text{Re}\, \tilde{g}(t) e^{j\omega_1 t} \tag{5}$$

where $\tilde{m}(t)$ and $\tilde{g}(t)$ are their respective complex envelopes.

[1] Bandpass realizations using stripline implementations have also been investigated [8].

Authorized licensed use limited to: Missouri University of Science and Technology. Downloaded on July 14,2023 at 19:42:27 UTC from IEEE Xplore. Restrictions apply.

With these representations, it can be shown that

$$\tilde{m}(t) = d(t) * \tilde{g}(t)$$
$$= d(t) * g_R(t) + jd(t) * g_I(t) \tag{6}$$

where $*$ denotes convolution and the subscripts R and I denote the real and imaginary parts, respectively, of the subscripted quantity. Using (6) in (4), we obtain

$$m(t) = d(t) * g_R(t) \cos \omega_1 t$$
$$- d(t) * g_I(t) \sin \omega_1 t \tag{7}$$

as the output of the serial MSK modulator.

Turning now to the parallel I/Q structure of Fig. 2(a), it follows directly from the block diagram that

$$m'(t) = d(t) * g_1(t) \cos (2\pi f_1 t)$$
$$+ d(t) * g_2(t) \sin (2\pi f_1 t). \tag{8}$$

The equivalence of the two structures requires that $m(t) = m'(t)$ which in turn requires that

$$g_1(t) = \operatorname{Re} \tilde{g}(t)$$
$$= g_R(t) \tag{9a}$$

and

$$g_2(t) = -\operatorname{Im} \tilde{g}(t)$$
$$= -g_I(t). \tag{9b}$$

It follows, therefore, that

$$\tilde{g}(t) = g_1(t) - jg_2(t) \tag{10}$$

and that the equivalent low-pass transfer function of the conversion filter is

$$\tilde{G}(f) \triangleq \mathcal{F}[\tilde{g}(t)]$$
$$= G_R(f) + jG_I(f)$$
$$= G_1(f) - jG_2(f) \tag{11}$$

where $\mathcal{F}[\cdot]$ denotes the Fourier transform and $G_R(f) = \mathcal{F}[g_R(t)]$, etc.

Now, from (1), the ideal conversion filter has impulse response

$$g(t) = \begin{cases} 2 \sin [2\pi(f_0 + 1/4T)t], & 0 \leqslant t \leqslant T \\ 0, & \text{otherwise} \end{cases}$$
$$= 2 \cos [2\pi(f_0 + 1/4T)t - \pi/2] \, \Pi(t/T - 0.5)$$
$$= \operatorname{Re} \{2 \exp [j2\pi(t/2T - 0.25)]$$
$$\cdot \exp [j2\pi(f_0 - 1/4T)t] \, \Pi(t/T - 0.5)\} \tag{12}$$

where $\Pi(t) \triangleq 1$, $-\frac{1}{2} \leqslant t \leqslant \frac{1}{2}$ and is zero otherwise. Equating (12) to (5) and separating $\tilde{g}(t)$ into its real and imaginary parts, we obtain

$$g_R(t) = \cos 2\pi(t/2T - 0.25)\Pi(t/T - 0.5)$$
$$= \sin (\pi t/T)\Pi(t/T - 0.5) \tag{13a}$$

and

$$g_I(t) = \sin 2\pi(t/2T - 0.25)\Pi(t/T - 0.5)$$
$$= -\cos (\pi t/T)\Pi(t/T - 0.5). \tag{13b}$$

The Fourier transforms of (13a) and of the negative of (13b) result in the transfer functions, $G_1(f)$ and $G_2(f)$, of the inphase and quadrature low-pass conversion filters of Fig. 2(a). By using the Fourier transform pair

$$\Pi(t/T) \leftrightarrow T \operatorname{sinc} (fT) \tag{14}$$

where $\operatorname{sinc}(u) \triangleq \sin(\pi u)/(\pi u)$ and appropriate Fourier transform theorems, we find these transfer functions to be

$$G_1(f) = 0.5T [\operatorname{sinc} (fT - 0.5)$$
$$+ \operatorname{sinc} (fT + 0.5)] \exp (-j\pi fT) \tag{15a}$$

and

$$G_2(f) = j0.5T [\operatorname{sinc} (fT - 0.5)$$
$$- \operatorname{sinc} (fT + 0.5)] \exp (-j\pi fT), \tag{15b}$$

respectively. From (11) and the expressions above for $G_1(f)$ and $G_2(f)$, the equivalent low-pass transfer function of the conversion filter is

$$G(f) = T \operatorname{sinc} (fT - 0.5) \exp (-j\pi fT) \tag{16}$$

These ideal conversion filter transfer functions are compared in Fig. 3. Note that the transfer function $G_1(f)$ of the inphase-arm filter is low-pass and an even function of frequency and that the transfer function $G_2(f)$ of the quadrature-arm filter is high-pass and an odd function of frequency. They add in phase quadrature to produce a bandpass conversion filter frequency response with even symmetry about the frequency $f_2 = f_0 + 1/4T$. (Recall that we have used $f_1 = f_0 - 1/4T$ as our reference frequency for the complex envelope representation so that f_1 corresponds to $fT = 0$ in the graphs of the low-pass equivalent transfer functions of Fig. 3.) The addition of $G_1(f)$ and $G_2(f)$ in phase quadrature produces the required bandpass equivalent transfer function. Approximations to these filters will be considered in Section III. Before discussing these approximations, we consider the low-pass equivalent for the matched filter of a serial MSK receiver.

C. Matched Filter Low-Pass Equivalents

The demonstration of equivalence of the serial MSK receiver structures of Figs. 1 and 2 proceeds similarly to that for the modulator. Since the details have been given in another

Authorized licensed use limited to: Missouri University of Science and Technology. Downloaded on July 14,2023 at 19:42:27 UTC from IEEE Xplore. Restrictions apply.

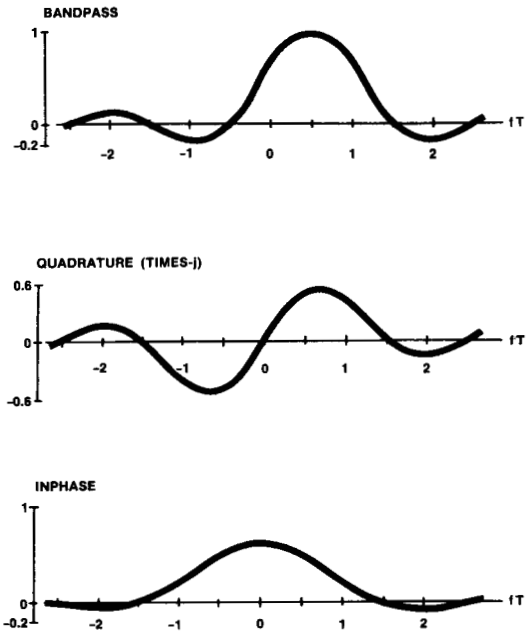

Fig. 3. Frequency response functions for serial MSK conversion filters.

paper [7], they will not be repeated here. Similar to the transmitter, the impulse responses of the inphase- and quadrature-arm matched filters of Fig. 2(b) are

$$h_1(t) = \mathrm{Re}\,\tilde{h}(t) \triangleq h_R(t) \tag{17a}$$

and

$$h_2(t) = -\mathrm{Im}\,\tilde{h}(t) \triangleq -h_I(t) \tag{17b}$$

where $\tilde{h}(t)$ denotes the complex envelope of the matched filter impulse response referenced to f_1. Thus, the real impulse response is

$$\begin{aligned} h(t) &= \mathrm{Re}\,\tilde{h}(t)e^{j\omega_1 t} \\ &= h_R(t)\cos\omega_1 t - h_I(t)\sin\omega_1 t. \end{aligned} \tag{18}$$

The spectrum of the complex envelope of an MSK signal, when referenced to the mark frequency, is [4]

$$\tilde{S}_{\mathrm{MSK}}(f) = \frac{4T}{\pi}\,\frac{\cos 2\pi(fT-0.25)}{1-16\,(fT-0.25)^2}. \tag{19}$$

Therefore, the transfer function of the low-pass equivalent MSK matched filter is

$$\tilde{H}(f) = \tilde{S}_{\mathrm{MSK}}(f)e^{-j2\pi f T_d} \tag{20}$$

where T_d is an arbitrary time delay. Using the Fourier transform pair

$$\cos(\pi t/2T)\Pi(t/2T) \leftrightarrow \frac{4T}{\pi}\,\frac{\cos(2\pi Tf)}{1-16(Tf)^2}$$

the complex envelope of the matched filter impulse response is found to be

$$\begin{aligned} \tilde{h}(t) &= \mathcal{F}^{-1}[\tilde{H}(f)] \\ &= \cos(\pi t/2T)\exp(j\pi t/2T)\Pi(t/2T) \quad (T_d \text{ assumed } 0) \end{aligned} \tag{21}$$

where T_d has been arbitrarily taken as zero. Separating (21) into its real and imaginary parts, we find that the impulse responses of the inphase- and quadrature-channel filters are

$$h_1(t) = h_R(t) = \cos^2(\pi t/2T)\Pi(t/2T) \tag{22a}$$

and

$$\begin{aligned} -h_2(t) &= h_I(t) \\ &= \cos(\pi t/2T)\sin(\pi t/2T)\Pi(t/2T). \end{aligned} \tag{22b}$$

The transfer functions of the inphase- and quadrature-channel filters, which are the Fourier transforms of (22), are

$$\begin{aligned} H_1(f) &= H_R(f) \\ &= \mathcal{F}[h_R(t)] \\ &= \frac{T}{2}\{2\,\mathrm{sinc}\,(2Tf) + \mathrm{sinc}\,(2Tf-1) + \mathrm{sinc}\,(2Tf+1)\} \end{aligned} \tag{23a}$$

and

$$\begin{aligned} -H_2(f) &= H_I(f) \\ &= \mathcal{F}[h_I(t)] \\ &= -j\frac{T}{2}\{\mathrm{sinc}\,(2Tf-1) - \mathrm{sinc}\,(2Tf+1)\}, \end{aligned} \tag{23b}$$

respectively. The transfer function of the low-pass equivalent matched filter can be found from

$$\tilde{H}(f) = H_R(f) + jH_I(f) = H_1(f) - jH_2(f) \tag{24}$$

and, as a check, shown to be the same as (19) with $T_d = 0$. The three transfer functions (19), (23a), and (23b) are compared in Fig. 4. As in the case of the conversion filter, $H_1(f)$ is even and real, $H_2(f)$ is imaginary and odd, and their quadrature sum is offset $0.25/T$ Hz from f_1, which is the reference frequency used for the low-pass equivalent representation. Furthermore, the low-pass transfer functions which are $2R$ wide between mainlobe zeros add in phase quadrature to produce a bandpass (or low-pass equivalent) transfer function which is $1.5R$ wide, where $R = 1/T$ is the data rate.

Authorized licensed use limited to: Missouri University of Science and Technology. Downloaded on July 14,2023 at 19:42:27 UTC from IEEE Xplore. Restrictions apply.

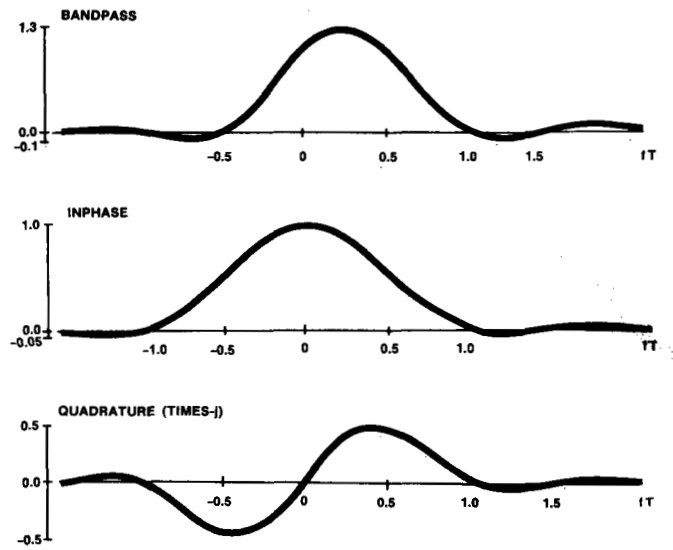

Fig. 4. Frequency response functions for the serial MSK matched filter.

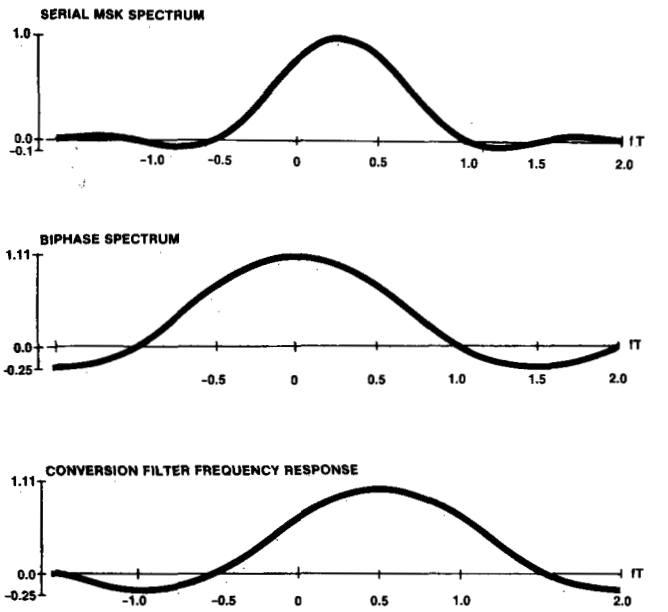

Fig. 5. Relationship between a serial MSK spectrum, the biphase spectrum and an ideal conversion filter frequency response.

III. CONVERSION FILTER APPROXIMATIONS

A. General Approach Using I/Q-Arm Filters with Periodic Frequency Responses

In this section, and in the following section where approximations for matched filters are considered, the approach of approximating the transfer function as a cascade of I/Q-arm filters with periodic frequency responses, to synthesize the mainlobe of the ideal response, and a bandlimiting filter to suppress the undesired lobes of the periodic response is employed.[2] Because of the symmetry of the I/Q modulator and demodulator structures, it follows that a configuration applicable for the modulator will work for the demodulator if the order of the components is reversed, and vice versa.

The maximum of the conversion filter frequency response must be offset from the maximum of the spectrum of the biphase modulator output one-half data rate as illustrated for the ideal case in Fig. 5. In Fig. 5, it will be noted that the left-hand zero ($fT = -0.5$) of the mainlobe of the conversion filter frequency response produces the left-hand zero in the serial MSK spectrum at $fT = -0.5$. On the other hand, the right-hand zero of the mainlobe of the MSK spectrum corresponds to the right-hand mainlobe zero of the biphase spectrum. It follows, therefore, that for any conversion filter approximation the left-hand side of the mainlobe is the most critical. (Note that the MSK spectrum could also be synthesized by interchanging the roles of the biphase spectrum and conversion filter frequency response of Fig. 5.)

B. Quadrature Hybrid Realizations

A quadrature hybrid is a four-part microwave device with transfer characteristics closely approximated by

$$H_{12}(f) = 0 \text{ (isolated port)} \tag{25a}$$

$$H_{13}(f) = \cos\theta \exp(-j\beta l) \text{ (dc port)} \tag{25b}$$

$$H_{14}(f) = j\sin\theta \exp(-j\beta l) \text{ (coupled port)} \tag{25c}$$

where

$\theta \cong \theta_{max} \sin \beta l$ (coupling angle)

$\beta l = 2\pi l/\lambda$

$\lambda = v/f =$ wavelength ($v =$ velocity of EM propagation in the coupling medium)

$l =$ physical coupling length (to be specified in dimensionless units of l/vT later)

$\theta_{max} =$ maximum coupling angle (geometry dependent).

In keeping with the discussion of Section III-A, we realize the mainlobe of the conversion filter frequency response of Fig. 3(c) with $H_{13}(f)$ and $H_{14}(f)$ in the inphase and quadrature arms, respectively, of the modulator structure of Fig. 2(a). With $G_1(f) = H_{13}(f)$ and $G_2(f) = H_{14}(f)$, the low-pass equivalent transfer function of the quadrature hybrid portion of the conversion filter becomes

$$\begin{aligned} G_{QH}(f) &= H_{13}(f) - jH_{14}(f) \\ &= (\cos\theta + \sin\theta)\exp(-j\beta l) \\ &= \sqrt{2}\cos(\theta - \pi/4)\exp(-j\beta l) \end{aligned} \tag{26}$$

where $\theta = \theta_{max} \sin(2\pi kfT)$, $k = l/vT$. The frequency response of this transfer function, scaled by $1/\sqrt{2}$, is illustrated in Fig. 6(a)-(c), respectively, for $\theta_{max} = 3\pi/8$, $\pi/8$, and $\pi/4$ with $k = 0.5$. The value $\theta_{max} = \pi/4$ appears best suited for matching the mainlobe of the ideal conversion filter frequency response shown in Fig. 3(a). With $k = 0.5$, the nulls of the

[2] Low-pass filters can also be used in the I/Q mixer arms or at the input to the modulator. From an implementation standpoint, it is desirable to have the sidelobe suppression filter at the output of the modulator to suppress spurious responses due to the I/Q-arm mixers and other nonlinearities.

Authorized licensed use limited to: Missouri University of Science and Technology. Downloaded on July 14,2023 at 19:42:27 UTC from IEEE Xplore. Restrictions apply.

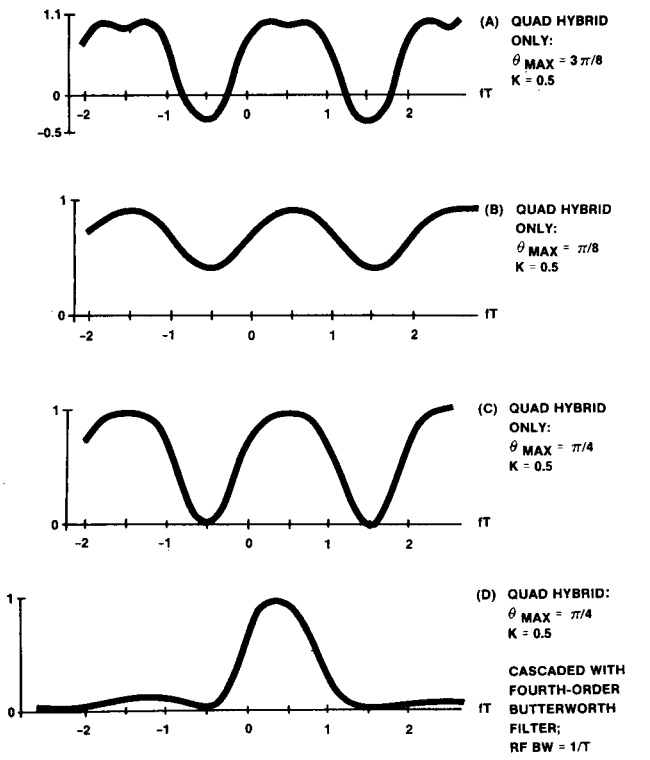

Fig. 6. Quadrature-hybrid implemented conversion filter frequency response.

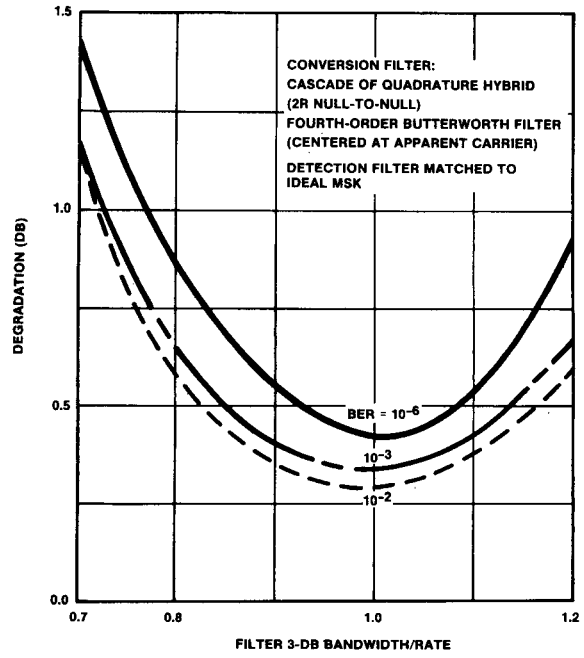

Fig. 7. Sensitivity of quadrature-hybrid implemented conversion filter to output filter bandwidth.

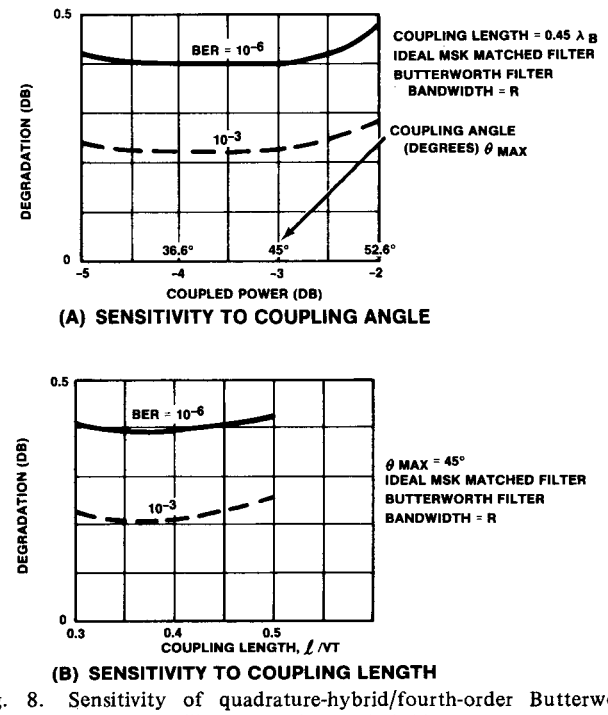

Fig. 8. Sensitivity of quadrature-hybrid/fourth-order Butterworth conversion filter to quadrature-hybrid parameters.

lobes of the quadrature hybrid frequency response are spaced two data rates, which is the same as for the ideal conversion filter. In order to suppress all lobes of the quadrature hybrid frequency response except the one around $f = 0$, a bandpass filter can be placed at the summer output, or low-pass filters can be used in the I/Q arms. Fig. 6(d) illustrates the overall frequency response obtained using a fourth-order Butterworth filter at the summer output of RF 3 dB bandwidth equal to one data rate. This bandwidth is chosen on the basis of the graphs of Fig. 7 which show degradation at various BER's as a function of filter bandwidth.

These results are obtained by a computer simulation which simulates the modem of Fig. 2 in response to the maximal-length pseudonoise sequence

0 1 0 0 1 0 0 0 0 1 0 1 0 1 1 1
0 1 1 0 0 0 1 1 1 1 1 0 0 1 1 0.

(A zero is added to balance the sequence.) The probability of error is computed for each bit of 29 bits by simulating the signal response and calculating the noise variance. (The results for the first two and last bits are excluded to avoid end effects.) The average of these error probabilities over the 29 bits is then computed.

Fig. 8 illustrates the sensitivity of the filter to quadrature hybrid coupling angle and coupling length. These results, which were also obtained by computer simulation, show that the detector performance is surprisingly insensitive to these two parameters.

This particular conversion filter realization is simple and satisfactory for high data rates. Furthermore, the fourth-order bandpass filter at the modulator output produces a spectrum with much lower sidelobe levels than an ideal MSK spectrum with only a moderate degradation from ideal. Fig. 9 shows plots of the power spectra for ideal MSK and quadrature-hybrid generated MSK for comparison.

C. Open/Shorted Transmission Line Realizations

Consider the open and shorted transmission lines driven by sources with internal impedance R_1 matched to the characteristic impedance of the line as shown in Fig. 10. The transfer

Authorized licensed use limited to: Missouri University of Science and Technology. Downloaded on July 14,2023 at 19:42:27 UTC from IEEE Xplore. Restrictions apply.

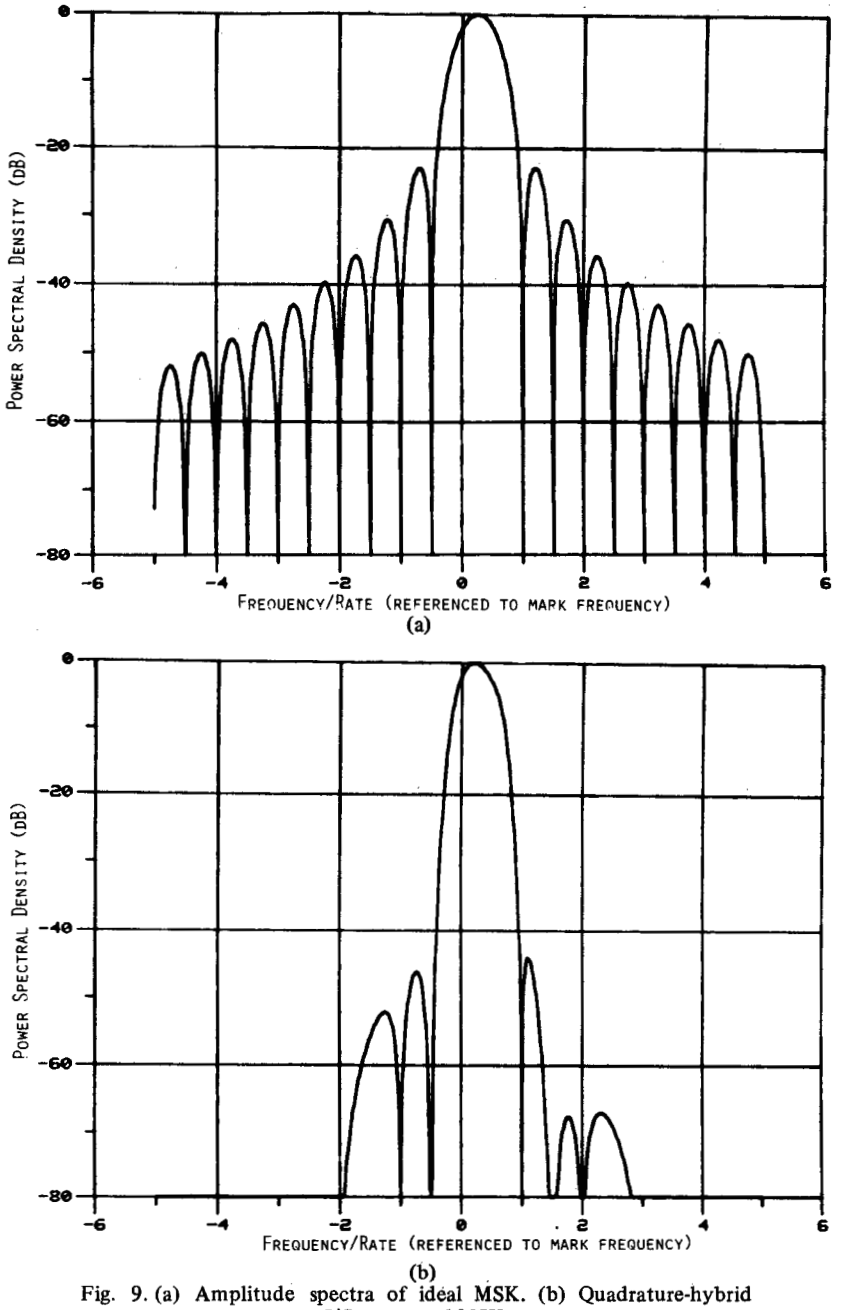

Fig. 9. (a) Amplitude spectra of ideal MSK. (b) Quadrature-hybrid I/Q generated MSK.

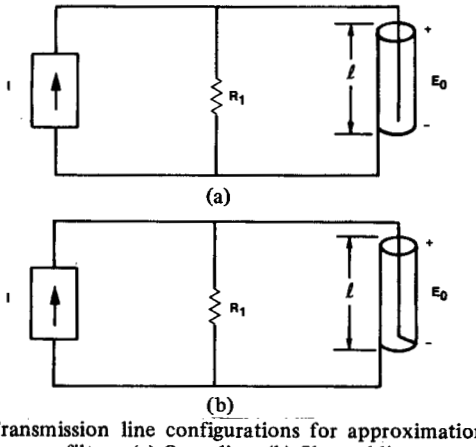

Fig. 10. Transmission line configurations for approximation of I/Q-arm filters. (a) Open line. (b) Shorted line.

function of this configuration is

$$H(\lambda) \triangleq \frac{E_0}{R_1 I} = \frac{1}{1 + R_1/Z_L} \tag{27}$$

where Z_L is the driving point impedance of the line. For the open line,

$$Z_L = -jZ_0 \cot \beta l \tag{28}$$

where $\beta = 2\pi/\lambda = 2\pi f/v$, v being the velocity of electromagnetic propagation on the line, and Z_0 the characteristic impedance of the line. For the shorted line

$$Z_L = jZ_0 \tan \beta l. \tag{29}$$

Authorized licensed use limited to: Missouri University of Science and Technology. Downloaded on July 14,2023 at 19:42:27 UTC from IEEE Xplore. Restrictions apply.

Therefore, if $R_1 = Z_0$, the transfer function of the open line configuration is

$$H_0(f) = \frac{1}{1 + j\tan(2\pi fl/v)}$$
$$= \cos(2\pi kfT)\exp(-j2\pi kfT) \tag{30}$$

and that of the shorted line configuration is

$$H_S(f) = \frac{1}{1 - j\cot(2\pi fl/v)}$$
$$= j\sin(2\pi kfT)\exp(-j2\pi kfT) \tag{31}$$

where $k = l/vT$ is the line delay in bit periods.

If an open line is used in the inphase arm of the I/Q modulator structure and a shorted line is used in the quadrature arm, the low-pass equivalent transfer function of this portion of the conversion filter is

$$G_{TL}(f) = H_0(f) - jH_s(f)$$
$$= [\cos(2\pi kfT) + \sin(2\pi kfT)]\exp(-j2\pi kfT)$$
$$= \sqrt{2}\cos(2\pi kfT - \pi/4)\exp(-j2\pi kfT). \tag{32}$$

If $k = 0.25$, the zeros of $G_{TL}(f)$ adjacent to $fT = 0$ match the mainlobe zeros of the ideal conversion filter frequency response. Suppression of the unwanted lobes of the periodic transfer function, given by (32), by a bandpass filter placed at the summer output then results in an approximation for the ideal conversion filter. Fig. 11 shows degradation of the SNR from ideal for various BER's as a function of filter 3 dB bandwidth for a fourth-order Butterworth filter at the summer output. These results, which were obtained by the computer simulation previously described, show that the optimum filter bandwidth is approximately one data rate. For a one data rate bandwidth, the degradation at a BER of 10^{-6} is about 0.43 dB, which is comparable to the quadrature-hybrid implemented conversion filter. The spectrum of the output of this conversion filter approximation is shown in Fig. 12. As in the case of the quadrature-hybrid conversion filter, the mainlobe of the spectrum shown in Fig. 12 closely approximates the mainlobe of the ideal MSK spectrum; however, the sidelobes are considerably lower.

E. Other Output Filters

Since the choice and placement of the output filter obviously has an effect on the spectrum and performance degradation, other combinations were tried, and some representative cases are presented here.

Degradation as a function of output filter bandwidth for the open/shorted transmission line structure with a third-order bandpass Butterworth filter at the summer output results in a minimum at about 0.7 data rates with a degradation at this bandwidth of roughly 0.7 dB at a BER of 10^{-6}. In addition to this larger degradation, the sidelobes of the transmitted signal spectrum are higher than for a fourth-order Butterworth filter due to the slower rolloff of attenuation with frequency. A plot of the spectrum is given in Fig. 13(a). For a second-order filter, yet a smaller optimum bandwidth results, with a corresponding larger degradation and higher spectral sidelobes.

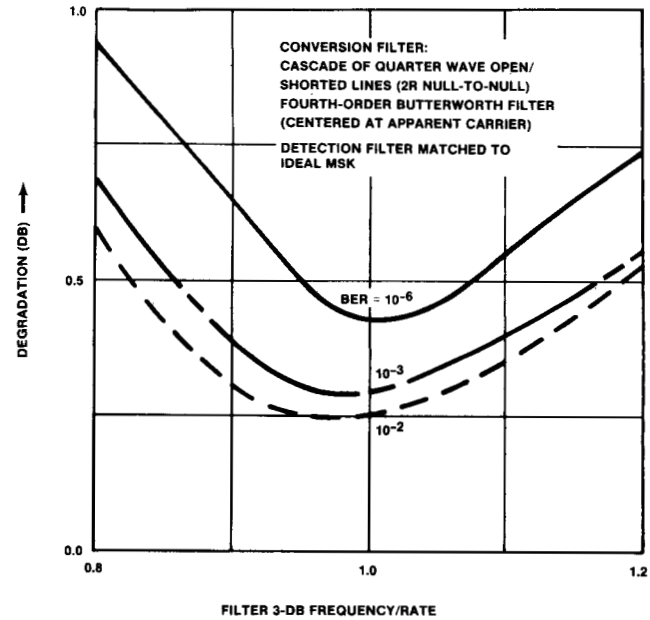

Fig. 11. Sensitivity of open/shorted line-implemented conversion filter to output filter bandwidth.

For a quadrature hybrid configuration with fourth-order low-pass Butterworth filters in each I/Q arm, or equivalently, at the data input to the modulator, the optimum low-pass bandwidth is roughly one data rate with a corresponding minimum degradation of about 0.35 dB. The minimum is very broad, however. Because of the sidelobe suppression filters being centered at the maximum of the BPSK spectrum rather than at the maximum of the modulator output spectrum, the sidelobes of the modulated signal spectrum are unsymmetrical as illustrated by Fig. 13(b), which shows a spectral plot for this filter combination.

Table I summarizes the optimum bandwidths and corresponding minimum degradations for the other filters examined, where optimum is in the sense of minimum degradation for an ideal MSK matched receiver. In general, a fourth-order filter at the summer output results in a low degradation and low sidelobe levels.

E. Envelope Deviation

Another important characteristic of the modulated signal produced by the I/Q modulator structure is the maximum-to-minimum deviation of its envelope. Fig. 14 shows envelope deviation as a function of output filter bandwidth for the quadrature hybrid and open/shorted transmission line I/Q modulator structures with a fourth-order Butterworth filter at the output. It is seen that for a filter bandwidth of one data rate, which corresponds to minimum BER degradation for an ideal MSK matched filter, the envelope deviation is about 3 dB, which corresponds to a maximum-to-minimum ratio of

Authorized licensed use limited to: Missouri University of Science and Technology. Downloaded on July 14,2023 at 19:42:27 UTC from IEEE Xplore. Restrictions apply.

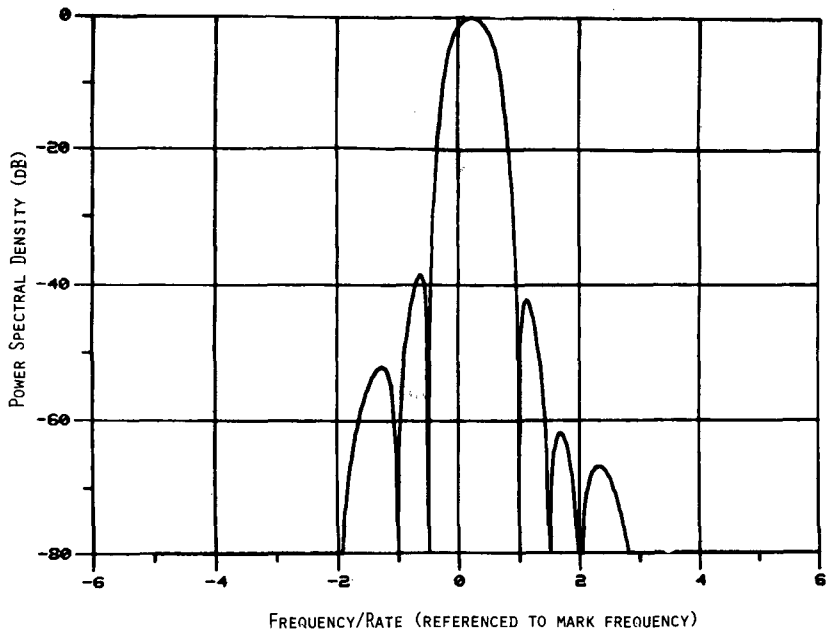

Fig. 12. Amplitude spectrum of I/Q-generated MSK (quarter wave open/shorted lines plus fourth-order Butterworth filter with RF bandwidth = R centered at apparent carrier).

1.4. The question of what happens to the spectrum when the modulator output signal is amplitude limited has not yet been examined.

Fig. 14 shows that lower envelope deviation is obtained as the output filter bandwidth is increased. However, for an MSK matched filter, the detector degradation also increases. To avoid this increased degradation, one may employ a detector matched to the transmitted signal. Simulations of such a detector have resulted in BER degradations of about 0.4 dB for output filter bandwidths greater than 1.2 data rates. Increasing the output filter bandwidth, of course, results in higher sidelobes on the transmitted signal spectrum.

IV. MATCHED FILTER APPROXIMATIONS

A. Realization with Transversal I/Q-Arm Filters

Using the same approach for the matched filter as for the conversion filter, we look for realizations for which the I/Q arm filters of Fig. 2(b) have a periodic frequency response, one period of which approximates the frequency response functions of the ideal I/Q-arm filters shown in Fig. 4. A second filter, either bandpass at the demodulator input or low-pass at the demodulator output, is used to suppress the unwanted lobes of this periodic frequency response. As illustrated in Fig. 4 and discussed in Section II, the inphase arm filter has a frequency response which is an even function of frequency, and the quadrature arm filter's frequency response is odd.

Realization of a periodic frequency response function can be accomplished with transversal, or tapped delay-line, filters. Whether or not the actual receiver would be built using transversal filters is immaterial at this point. We are simply using this approach to aid our intuition.

The block diagram of a general transversal filter I/Q demodulator structure is shown in Fig. 15. Fig. 16 illustrates the low-pass equivalent frequency response of such a structure followed by a low-pass filter, designated as LPF 2, at the summer output. Because the quadrature sum of the frequency responses of the I/Q-arm filters is ideally offset from zero frequency by one-fourth data rate, LPF 2 attenuates the undesired positive- and negative-frequency lobes of this periodic frequency response unsymmetrically. Thus, optimization of the bandwidth of LPF 2 implies a tradeoff between attenuation of these undesired sidelobes and distortion of the desired central lobe of the periodic frequency response.

We now consider two transversal detection filter structures to illustrate this tradeoff. The first of these can be realized with the open/shorted transmission line approach discussed in regard to the conversion filter. A lumped-element approximation to the transversal detection filter will also be considered. The use of a quadrature hybrid to realize the periodic frequency response will not be discussed here because its performance characteristics have been reported in a previous paper [9].

B. Single-Delay Structure (Delay-Line Structure 1)

The simplest transversal filter structure consists of a single delay. The delayed and undelayed outputs are summed to realize a filter with an even frequency response; they are differenced to realize a filter with an odd frequency response.

Using the fact that the transfer function of a delay of T_d seconds is $\exp(-j2\pi f T_d)$, the transfer function of the inphase-arm filter is

$$H_1(f) = 2\cos(\pi b f T)\exp(-j\pi b f T) \tag{33}$$

and that of the quadrature-arm filter is

$$H_2(f) = 2j\sin(\pi b f T)\exp(-j\pi b f T) \tag{34}$$

Authorized licensed use limited to: Missouri University of Science and Technology. Downloaded on July 14,2023 at 19:42:27 UTC from IEEE Xplore. Restrictions apply.

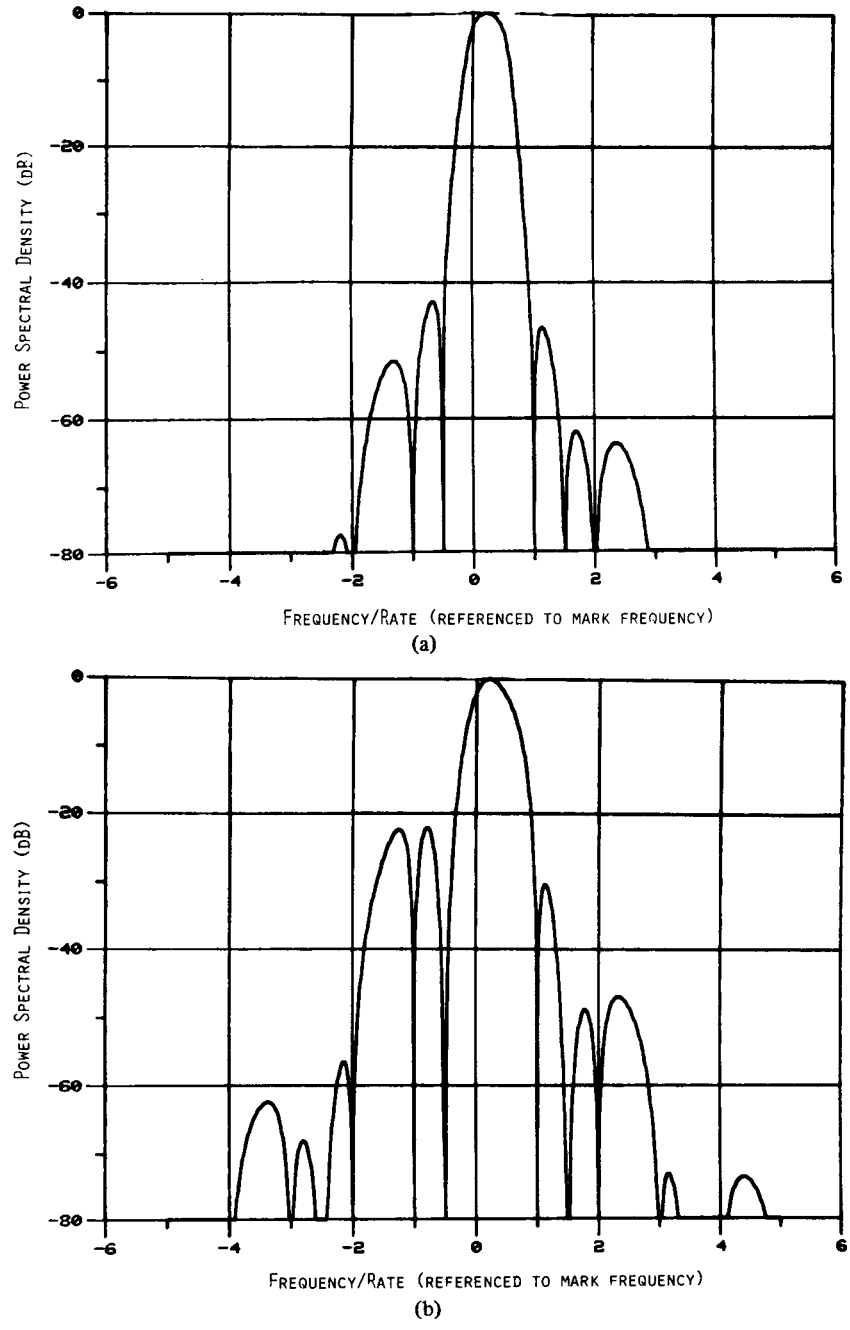

Fig. 13. Amplitude spectra of I/Q-generated MSK. (a) Quarter wave open/shorted lines plus third-order Butterworth with RF bandwidth = $0.7R$ centered at apparent carrier. (b) Quadrature hybrid plus low-pass filters with bandwidth = R prior to I/Q mixers.

Authorized licensed use limited to: Missouri University of Science and Technology. Downloaded on July 14,2023 at 19:42:27 UTC from IEEE Xplore. Restrictions apply.

TABLE I
OPTIMUM BANDWIDTHS, DEGRADATIONS, AND ENVELOPE DEVIATIONS FOR VARIOUS MODULATOR BANDLIMITING FILTER COMBINATIONS

I/Q ARM FILTER	BUTTERWORTH FILTER ORDER	FILTER PLACEMENT	OPTIMUM BANDWIDTH*	Degradation (dB): BER=10^{-6}	BER=10^{-3}	ENVELOPE DEVIATION(dB)
Quadrature Hybrid	2	Pre-mixer	1.2R; low-pass	0.33	0.17	3.6
Open/Shorted Lines	2	Pre-mixer	1.25R; low-pass	0.31	0.15	3.4
Quadrature Hybrid	2	Post-summer	0.55R; band-pass	0.84	0.61	3.5
Quadrature Hybrid	3	Pre-mixer	R; low-pass	0.30	0.14	3.0
Open/Shorted Lines	3	Post-summer	0.7R; band-pass	0.73	0.41	3.5
Quadrature Hybrid	4	Pre-mixer	R; low-pass	0.31	0.14	2.9
Quadrature Hybrid	4	Post-summer	R; bandpass	0.41	0.23	2.7
Open/Shorted Lines	4	Post-summer	R; bandpass	0.40	0.22	3.1

*Optimum in the sense of minimum degradation for a receiver matched to an ideal MSK signal.

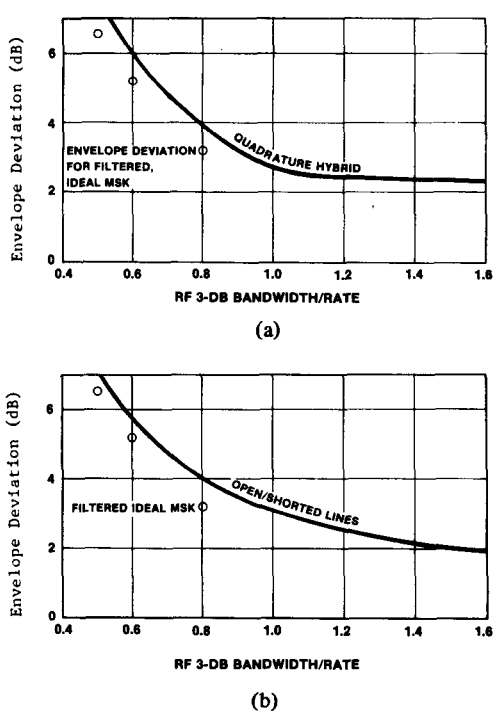

Fig. 14. Envelope deviation for I/Q modulators as a function of output filter bandwidth (fourth-order Butterworth filter at summer output and at ideal MSK modulator output). (a) Quadrature-hybrid (b) Open/shorted transmission lines.

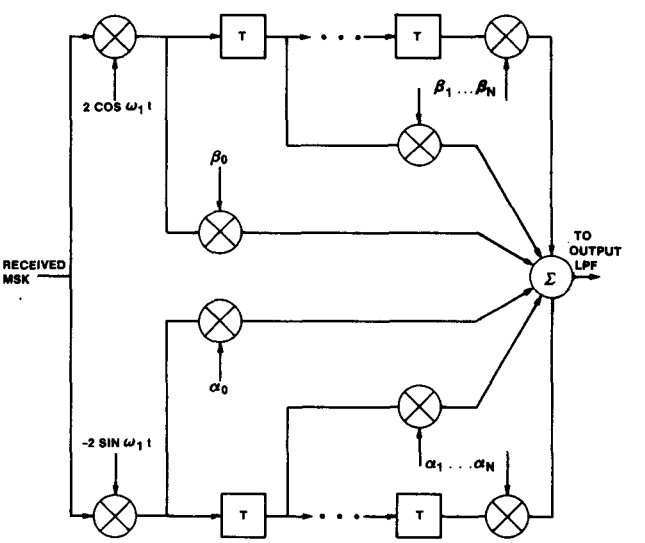

Fig. 15. Transversal filter structure for detection of MSK.

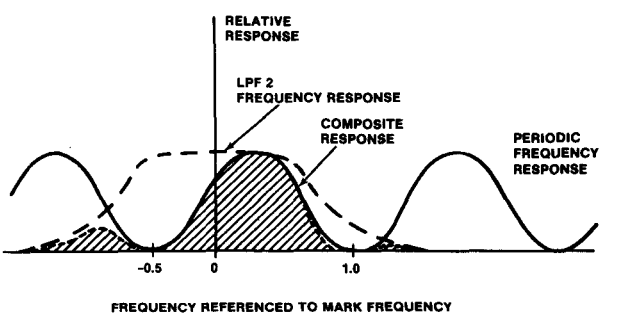

Fig. 16. Frequency response functions illustrating the approximation of ideal MSK matched filter response.

Authorized licensed use limited to: Missouri University of Science and Technology. Downloaded on July 14,2023 at 19:42:27 UTC from IEEE Xplore. Restrictions apply.

where $b = T_d/T$ is the delay in the I-and Q-arms in bit periods. Comparison of (33) and (34) with (30) and (31), respectively, shows that the single-delay structures considered here can be realized by the open/shorted transmission line approach discussed previously in regard to the conversion filter. This is not surprising since an ideal transmission line is characterized by pure delay.

Combining (33) and (34) according to (24), we find the transfer function of the low-pass equivalent matched filter for this implementation to be

$$\tilde{H}_a(f) = 2\sqrt{2}\cos[\pi(bfT - 0.25)]\exp(-j\pi bfT). \tag{35}$$

A sketch of the magnitude of (35) shows that its zeros adjacent to the origin are at $-1/4b$ and $3/4b$, and that the maximum for this period is at $1/4b$. In terms of matching the mainlobe of the ideal matched filter response of Fig. 4(a), no completely satisfactory choice for b exists. For example, if the distance between zeros of the mainlobe of the ideal is matched with the distance between the central lobe zeros of the approximation $b = 2/3$ results, which places the central lobe maximum at $f = 3/8T$, whereas the maximum of the ideal response is at $f = 1/4T$.

In order to obtain more flexibility in matching the periodic frequency response implemented by the I/Q-arm transversal filter to the ideal, we consider the two-delay case next.

C. Double-Delay Structure (Delay-Line Structure 2)

Considering the case of two delays in each arm of Fig. 15, we find the I- and Q-arm transfer functions to be

$$\begin{aligned} H_1(f) &= \beta_0 + \beta_1 e^{-j2\pi fT_d} + \beta_2 e^{-j4\pi fT_d} \\ &= (\beta_0 e^{j2\pi fT_d} + \beta_1 + \beta_2 e^{-j2\pi fT_d})e^{-j2\pi fT_d} \end{aligned} \tag{36}$$

and

$$\begin{aligned} H_2(f) &= \alpha_0 + \alpha_1 e^{-j2\pi fT_d} + \alpha_2 e^{-j4\pi fT_d} \\ &= (\alpha_0 e^{j2\pi fT_d} + \alpha_1 + \alpha_2 e^{-j2\pi fT_d})e^{-j2\pi fT_d}, \end{aligned} \tag{37}$$

respectively. Imposing the restrictions that $H_1(f)$ be an even function of frequency and $H_2(f)$ odd, excluding the linear phase factor, we require that

$$\beta_0 = \beta_2 = 1 \text{ (without loss of generality)} \tag{38a}$$

$$\alpha_1 = 0 \tag{38b}$$

$$\alpha_0 = -\alpha_2 \triangleq \alpha. \tag{38c}$$

With these restrictions, $H_1(f)$ and $H_2(f)$ can be rewritten as

$$H_1(f) = [\beta + 2\cos(2\pi bfT)]\exp(-j2\pi bfT) \tag{39}$$

and

$$H_2(f) = 2j\alpha\sin(2\pi bfT)\exp(-j2\pi bfT) \tag{40}$$

where $b = T/T_d$ is the delay in bit periods as before.

Although the parameters α and β conceivably could be optimized in the sense of minimizing degradation by computer simulation, some forethought considerably shortens this procedure. Observation of Fig. 4(a) suggests that a cosine-squared frequency response offset from the origin by one-fourth data rate will closely approximate the mainlobe of the ideal matched filter frequency response. We therefore substitute (39) and (40) into (24) to obtain

$$\begin{aligned} H_b(f) &= [\beta + 2\cos(2\pi bfT) \\ &\quad + 2\alpha\sin(2\pi bfT)]\exp(-j2\pi bfT) \\ &= \cos^2(\pi bfT - \theta/2)\exp(-j2\pi bfT) \end{aligned} \tag{41}$$

where

$$\theta = \tan^{-1}(\alpha) \tag{42}$$

and impose the additional condition

$$\beta = 2\sqrt{1+\alpha^2} = \tfrac{1}{2} \tag{43}$$

to obtain the cosine-squared form and normalize the maximum value to unity.

If the magnitude of the ideal matched filter frequency response is normalized to unity, then its value at the mark and space frequencies is $\pi/4$. By matching the transversal and matched filter frequency responses, suitably normalized, at the mark frequency (i.e., $fT = 0$), we obtain the condition

$$\theta = 2\cos^{-1}\sqrt{\pi/4}. \tag{44}$$

The additional condition that the maximum occurs at $fT = 0.25$ results in

$$b = 2\theta/\pi. \tag{45}$$

A comparison of the mainlobes of the ideal and approximate frequency responses, given in Fig. 17, shows that the mainlobes of the approximate and ideal responses are virtually identical if the conditions (44) and (45) are imposed. However, the output low-pass filter affects the overall response. In order to optimize the overall response of the transversal and low-pass filter cascade, a somewhat smaller normalized delay than given by (45) is required. Simulation of this detection filter with an ideal MSK input indicates the optimized delays and low-pass filter 3 dB frequencies given in Table II.

Degradations for other parameter values are provided in another paper [7].

D. Lumped-Element Approximations

As a means for realizing an I/Q form of matched filter at lower data rates, consider the lumped-element circuit shown in Fig. 18. The crisscrossed $L_1 - C_1$ elements realize the large central lobe of the MSK spectrum, while the output low-pass filters composed of L_2, C_2, and R attenuate the higher frequency lobes. While tedious to analyze, computer simulations

Authorized licensed use limited to: Missouri University of Science and Technology. Downloaded on July 14,2023 at 19:42:27 UTC from IEEE Xplore. Restrictions apply.

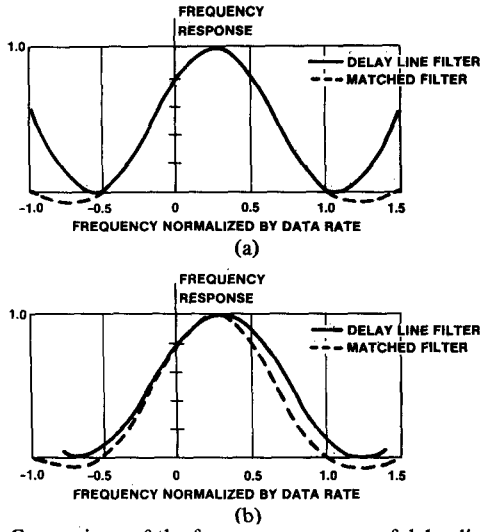

Fig. 17. Comparison of the frequency response of delay-line structure 2 with the frequency response of the matched filter for MSK. (a) Delay = $0.613T$. (b) Delay = $0.53T$. Third-order Butterworth output filter.

TABLE II
OPTIMUM DELAYS AND 3 dB FREQUENCIES FOR TRANSVERSAL FILTER DETECTOR

Type of Output Filter	Optimum 3 dB Bandwidth	Optimum Delay	Degradation at BER = 10^{-6}
Third-order Butterworth	$0.7/T$	$0.53T$	0.27 dB
Fifth-order Butterworth	$0.8/T$	$0.58T$	0.32 dB

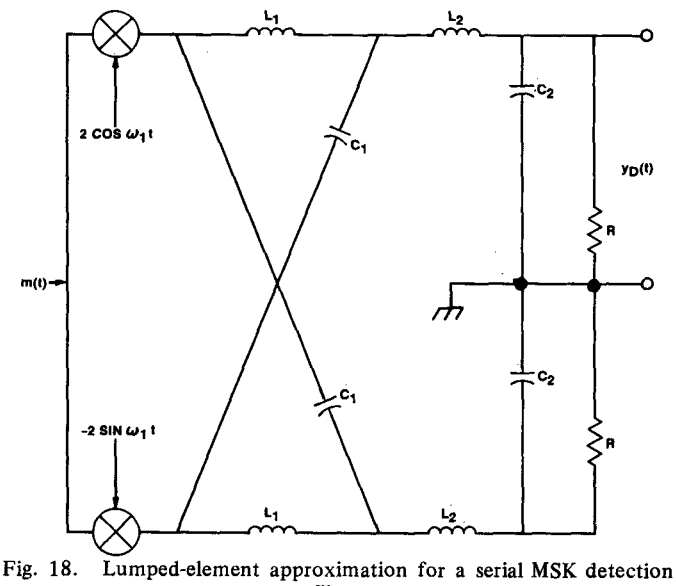

Fig. 18. Lumped-element approximation for a serial MSK detection filter.

have shown that very good approximations to the MSK matched filter can be obtained.

The frequency response function shown in Fig. 19 corresponds to the following normalized element values for the circuit of Fig. 18:

$L_1 = 2.5$ $\quad L_2 = 16$

$C_1 = 0.0045$ $\quad C_2 = 0.006.$

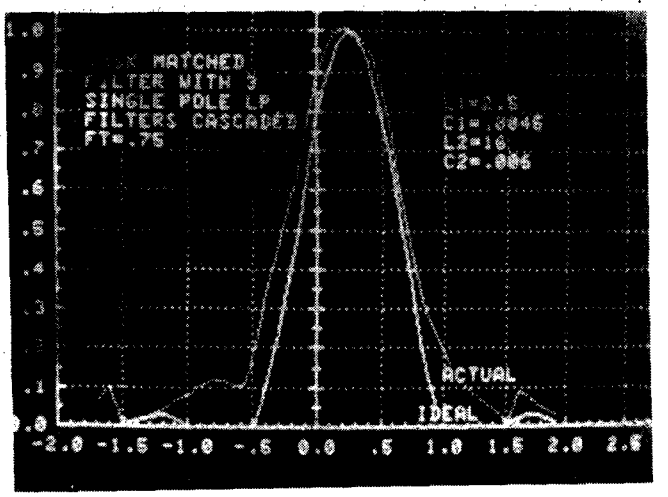

Fig. 19. Lumped-element detection filter frequency response.

TABLE III

3 dB Bandwidth 1-pole cascade (Hz)	Degradation (dB) BER = 10^{-6}
$0.5/T$	0.8
$0.75/T$	0.38
$1/T$	0.41

The normalizations $R = \sqrt{L/C}$ and $T_d = \sqrt{LC} = T$ have been used. A cascade of three 1-pole filters follow the crisscrossed LC filter. This cascade represents the low-pass filters inherent in the mixers, summers and isolation amplifiers. The degradations for several bandwidths of this 1-pole cascade are tabulated in Table III.

Other parameter values and configurations result in comparable degradations. For example, a double crisscross section filter gives about the same degradation as a single crisscross section when the parameters of both are optimized. Because of the lower number of elements, the single crisscross is preferable.

V. HARDWARE PERFORMANCE

The previous sections have provided theoretical, as well as simulated, results for implementation of serial modulators and demodulators. In this section, the performance of one of the many different types of modulator conversion filters is demonstrated, namely, the quadrature hybrid implementation. The block diagram of Fig. 20 illustrates the test setup. A 500 Mbit/s pseudorandom code is used as the data source with a quadrature hybrid having normalized coupling length of $l/vT = k = 0.625$, and a two-pole post-modulation Butterworth filter with a 3 dB bandwidth of 560 MHz or $1.12\,R$. These values were used because of availability of components. The carrier frequency is 3.3 GHz.

Fig. 21 illustrates the envelope amplitude and power spectral density of the signal at various points in the modulation and filtering process. Note that the envelope deviation is about 3.5 dB. With a more optimal selection of k and filter bandwidth, this can be reduced to under 3 dB in accordance with the simulation results of Table I, and the asymmetry of the

Authorized licensed use limited to: Missouri University of Science and Technology. Downloaded on July 14,2023 at 19:42:27 UTC from IEEE Xplore. Restrictions apply.

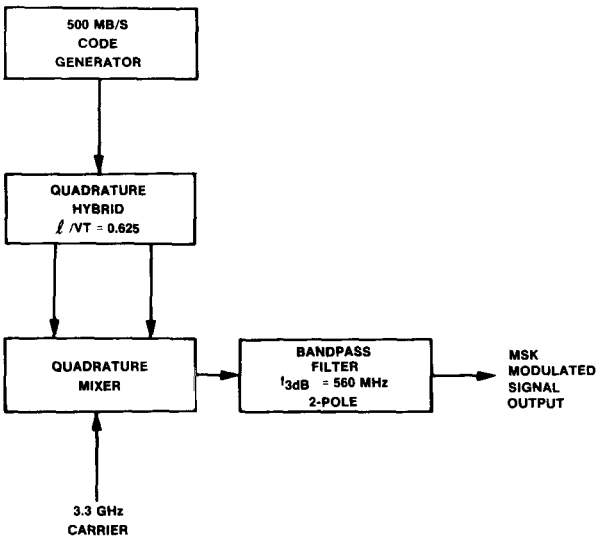

Fig. 20. SMSK modulator test configuration.

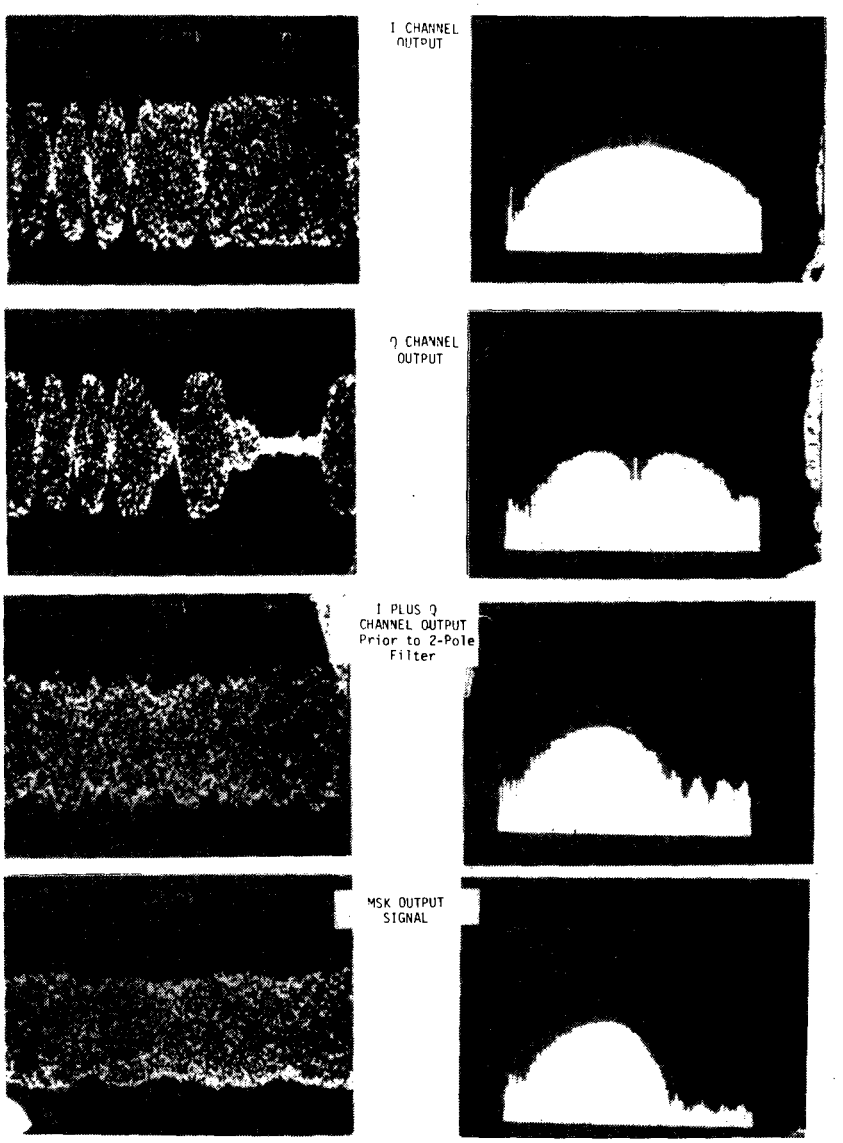

Fig. 21. Envelope and power spectral densities for a quadrature-hybrid implemented serial MSK modulator. All time domain waveforms are at 2 ns per division horizontal and linear vertical scale. All frequency domain signals are at 100 MHz per division horizontal and 10 dB per division vertical.

Authorized licensed use limited to: Missouri University of Science and Technology. Downloaded on July 14,2023 at 19:42:27 UTC from IEEE Xplore. Restrictions apply.

final MSK output spectrum would also be decreased. The effects of this assymmetry on system degradation can be minimized through proper design of the detection filter.

VI. CONCLUSION

Serial MSK modulation and demodulation is ideally suited to high data rate applications requiring constant-envelope signals with moderate bandwidth efficiency provided that realizations of the conversion and matched filters can be found which impose low degradation. The low-pass parallel inphase/quadrature channel structures considered here have several advantageous implementation features. Several possible realization techniques have been characterized in terms of SNR degradation and shown to depart only about 0.5 dB or less from ideal when optimized.

ACKNOWLEDGMENT

The assistance of D. Dolan and R. Bohn in optimizing and providing computer results for the lumped-element detection filters is appreciated.

REFERENCES

[1] R. de Buda, "Coherent demodulation of frequency-shift keying with low deviation ratio," *IEEE Trans. Commun.*, vol. COM-20, pp. 429–435, June 1972.
[2] S. A. Gronemeyer and A. L. McBride, "MSK and offset QPSK modulation," *IEEE Trans. Commun.*, vol. COM-24, pp. 809–820, Aug. 1976.
[3] F. Amoroso and J. A. Kivett, "Simplified MSK signaling technique," *IEEE Trans. Commun.*, vol. COM-25, pp. 433–441, Apr. 1977.
[4] S. Pasupathy, "Minimum shift keying: A spectrally efficient modulation," *IEEE Commun. Mag.*, vol. 17, pp. 14–22, July 1979.
[5] C. R. Ryan, A. R. Hambley, and D. E. Vogt, "760 Mbit/s serial MSK microwave modem," *IEEE Trans. Commun.*, vol. COM-28, pp. 771–777, May 1980.
[6] W. R. Smith, "SAW filters for CPSM spread spectrum communication," in *Proc. Nat. Telecommun. Conf.*, Nov. 1980, pp. 22.2.1–22.2.6.
[7] R. E. Ziemer and C. R. Ryan, "Near optimum delay-line detection filters for serial detection of MSK signals," in *Proc. Int. Conf. Commun.*, June 1981, pp. 56.2-1–56.2-5.
[8] D. J. Rasmussen, "Generation of serial MSK signals with non-ideal conversion filters," M.S. thesis, Dep. Elec. Eng., Arizona State Univ., Tempe, AZ, May 1981.
[9] J. M. Liebetreu and C. R. Ryan, "Performance simulation of receiver filters for serial detection of MSK signals," in *Allerton Conf. Proc.*, Oct. 1980, pp. 351–358.

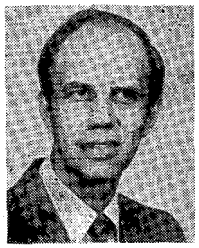

Rodger E. Ziemer (S'60–M'66–SM'70) was born in Sargeant, MN, on August 22, 1937. He received the B.S., M.S.E.E., and Ph.D. degrees from the University of Minnesota, Minneapolis, in 1960, 1962, and 1965, respectively.

He has been on the faculty of the University of Missouri–Rolla (UMR) since 1968, where he is currently Professor of Electrical Engineering. In addition to teaching courses and performing research in communications and signal processing, he has been a Consultant with several industries and government agencies on problems involving signal processing in communications and radar systems. During the academic year 1980–1981 he was on leave from UMR while doing research and development on high data-rate communications systems at the Communications Research Facility of Motorola Government Electronics Division at Scottsdale, AZ.

Dr. Ziemer has published numerous papers in his areas of research interest and has coauthored a textbook entitled *Principles of Communications: Systems, Modulation, and Noise* (Boston, MA: Houghton-Mifflin). He is a member of Tau Beta Pi, Eta Kappa Nu, Sigma Xi, the American Society for Engineering Education, and is a Registered Professional Engineer.

★

Carl R. Ryan (S'61–M'62–SM'77) was born in Gateway, AR, on March 3, 1938. He received the B.S., M.S., and Ph.D. degrees in electrical engineering from the University of Arkansas, Fayetteville, Iowa State University, Ames, and the University of Missouri–Rolla, in 1962, 1963, and 1969, respectively.

He has been with the Motorola Government Electronics Division at Scottsdale, AZ, since 1963 and involved in various aspects of high data rate signal processing and communications systems. During the period of 1977 to 1979, he was on the faculty at Michigan Technological University, Houghton, as a Professor of Electrical Engineering. He is currently Manager of the Communications Research Facility of Motorola.

Dr. Ryan has published numerous articles and papers and holds six patents relating to communication signal processing and high data rate circuit and system design. He is a member of Eta Kappa Nu, Sigma Xi, and Phi Kappa Phi.

★

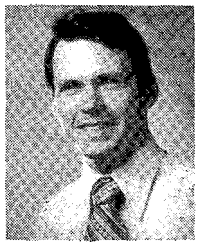

James H. Stilwell (S'72–M'74) was born in Olney, IL, on October 8, 1942. He received the B.S., M.S., and Ph.D degrees in electrical engineering from the University of Illinois, Urbana, Southern Methodist University, Dallas, TX, and Arizona State University, Tempe, in 1965, 1969, and 1974, respectively.

From 1965 until 1969 he was a Design Engineer with the Government Products Division of Texas Instruments. Since 1969 he has been with the Government Electronics Division of Motorola in Scottsdale, AZ, where he has been involved in communications systems and wide-band signal processing.

Authorized licensed use limited to: Missouri University of Science and Technology. Downloaded on July 14,2023 at 19:42:27 UTC from IEEE Xplore. Restrictions apply.